International Journal of Infectious Diseases 123 (2022) 145–156

Contents lists available at ScienceDirect

International Journal of Infectious Diseases

journal homepage: www.elsevier.com/locate/ijid

Mask disinfection using atmospheric pressure cold plasma

Ana Sainz-García[1], Paula Toledano[2], Ignacio Muro-Fraguas[1], Lydia Álvarez-Erviti[3], Rodolfo Múgica-Vidal[1], María López[2], Elisa Sainz-García[1], Beatriz Rojo-Bezares[2], Yolanda Sáenz[2,#,**], Fernando Alba-Elías[1,#,*]

[1] Department of Mechanical Engineering, University of La Rioja, C/ San José de Calasanz 31, 26004 Logroño, La Rioja, Spain
[2] Molecular Microbiology Area, Center for Biomedical Research of La Rioja (CIBIR), C/Piqueras 98, 26006 Logroño, La Rioja, Spain
[3] Molecular Neurobiology Area, Center for Biomedical Research of La Rioja (CIBIR), C/Piqueras 98, 26006 Logroño, La Rioja, Spain

ARTICLE INFO

Article history:
Received 29 June 2022
Revised 12 August 2022
Accepted 14 August 2022

Keywords:
Cold plasma
Plasma treatment
Mask
Antibacterial treatment
Disinfection

ABSTRACT

Objectives: Mask usage has increased over the last few years due to the COVID-19 pandemic, resulting in a mask shortage. Furthermore, their prolonged use causes skin problems related to bacterial overgrowth. To overcome these problems, atmospheric pressure cold plasma was studied as an alternative technology for mask disinfection.

Methods: Different microorganisms (*Pseudomonas aeruginosa, Escherichia coli, Staphylococcus* spp.), different gases (nitrogen, argon, and air), plasma power (90-300 W), and treatment times (45 seconds to 5 minutes) were tested.

Results: The best atmospheric pressure cold plasma treatment was the one generated by nitrogen gas at 300 W and 1.5 minutes. Testing of breathing and filtering performance and microscopic and visual analysis after one and five plasma treatment cycles, highlighted that these treatments did not affect the morphology or functional capacity of the masks.

Conclusion: Considering the above, we strongly believe that atmospheric pressure cold plasma could be an inexpensive, eco-friendly, and sustainable mask disinfection technology enabling their reusability and solving mask shortage.

Introduction

Masks that cover the nose and mouth are one of the main barriers to avoid the acquisition and transmission of microbial diseases, reducing viral transmission by 95% (Catching *et al.*, 2021; Feng *et al.*, 2020; Ng *et al.*, 2020; Suess *et al.*, 2012). During the last few years, the use of masks has increased due to the COVID-19 pandemic (Feng *et al.*, 2020). However, 93.64% of individuals hadskin reactions, like itching, stinging, dryness, and acne after mask exposure (Choi *et al.*, 2021; Damiani *et al.*, 2021). Maskne (mask+acne) is considered as the skin disease that provokes the highest number of dermatologist visits, and it could be aggravated by sebum, increase in pH, changes in CO_2 levels, and skin humidity (Choi *et al.*, 2021; Damiani *et al.*, 2021; Hua *et al.*, 2020; Kutlu *et al.*, 2020; Mutalik and Inamdar, 2020). These conditions favor the growth and proliferation of specific skin bacteria that cause respiratory diseases (Bao *et al.*, 2020; Choi *et al.*, 2021; Wei *et al.*, 2021). Daou *et al.* (2021) found that *Cutibacterium acnes* is the main bacterium responsible for maskne; however, other bacteria such as *Staphylococcus aureus, Staphylococcus epidermidis,* and *Escherichia coli* can also cause the disease (Daou *et al.*, 2021; Jusuf *et al.*, 2020; Sun and Chang, 2017). These problems are exacerbated by the prolonged use of masks during the COVID-19 pandemic because of mask shortage (Dharmaraj *et al.*, 2021; Feng *et al.*, 2020). Thus, correct and secure mask reuse is fundamental to reduce the consumption of manufacturing resources, facilitate the management of biological residues, and hence protect the environment. Masks are made of nondegradable plastic material, most of which ends up in the oceans and causes damage to the ecosystem (Dharmaraj *et al.*, 2021). However, not only recycling but also the destruction of the pathogens of the mask is important to reduce environmental pollution and the spread of microbial diseases

* Corresponding authors: Fernando Alba-Elías, Department of Mechanical Engineering, University of La Rioja, c/ San José de Calasanz 31, 26004, Logroño, La Rioja, Spain, Tel.: +34 941299276
** Corresponding authors: Yolanda Sáenz, Molecular Microbiology Area, Center for Biomedical Research of La Rioja (CIBIR), c/ Piqueras 98, 26006, Logroño, La Rioja, Spain, Tel.: +34 941278868
E-mail addresses: ysaenz@riojasalud.es (Y. Sáenz), fernando.alba@unirioja.es (F. Alba-Elías).
# These authors contributed equally to this work.

https://doi.org/10.1016/j.ijid.2022.08.012

(Dharmaraj *et al.*, 2021; Sangkham, 2020). In short, mask disinfection promotes environmental sustainability.

Researchers worldwide have studied mask disinfection systems against viruses and bacteria during the COVID-19 pandemic (Battelle, 2016; Cassorla, 2021; Heimbuch *et al.*, 2011; Kenney *et al.*, 2020; Lin *et al.*, 2018, 2017; Lore *et al.*, 2012; Mills *et al.*, 2018). A previous study investigated different mask decontamination methods (bleach, UV irradiation, autoclave, dry heating), achieving complete inactivation of *Bacillus subtilis* spores (Lin *et al.*, 2018). Another study analyzed different methods (UV radiation, dry heat, 70% ethanol, and vaporized hydrogen peroxide [VHP]) to reduce SARS-CoV-2 infection. The greatest inactivation results were obtained with VHP, which maintained the filtration characteristics even after three treatment cycles (Fischer *et al.*, 2020).

Other researchers have also pointed out the functional degradation of masks and the presence of residues after ethanol, UV irradiation, blenching, microwave heating, or VHP treatments (Battelle, 2016; Bergman *et al.*, 2010; Smith *et al.*, 2020; Viscusi *et al.*, 2009).

Low-temperature plasmas have been used for mask disinfection, with hydrogen peroxide gas plasma technology being the most widely used. Most authors have used the Sterrad 100NX plasma generator, which requires a vacuum atmosphere and long treatment times (Ibáñez-Cervantes *et al.*, 2020; Kumar *et al.*, 2020; Viscusi *et al.*, 2009; Wigginton *et al.*, 2021). Viscusi *et al.* (2009) analyzed mask deterioration after a 55 minutes of hydrogen peroxide gas plasma treatment and observed no negative impact either on filter aerosol or on filter airflow resistance. In some studies, more than one cycle of hydrogen peroxide gas plasma treatment affected the filtration and breathing capacity of masks (Bergman *et al.*, 2010; Kumar *et al.*, 2020; Wigginton *et al.*, 2021).

In this regard, atmospheric pressure cold plasma (APCP) technology has been a focus of increased research in recent years for disinfection applications. The most important investigations on the use of APCP for mask disinfection have been examined to further elaborate on the novelty of the current study, which, in conclusion, is scarce in the literature. Indeed, to our knowledge, there are only two publications. In the first publication, a dielectric barrier discharge plasma generator was used to generate ozone to treat KF94 mask portions (30 × 35 mm size) at different durations (10-300 seconds) against virus and bacteria (Lee *et al.*, 2021). The authors observed a total inactivation of *S. aureus* (10 seconds). Neither the structural characteristics of the filter layer nor the functional properties of the mask altered negatively after five 60-second treatment cycles in KF94 masks. In the second publication, plasma was generated using a dielectric barrier discharge plasma equipment to treat SARS-CoV-2 inoculated on N95/ filtering face piece 2 (FFP2) and N99/ filtering face piece 3 (FFP3) mask portions (4 × 4 cm size). No significant negative effect was detected on filtration efficiencies. Plasma was characterized by analyzing the optical emission spectrum, and it was observed that reactive oxygen and nitrogen species (RONS) such as OH*, NO, and ozone had a viricidal effect (Kim *et al.*, 2021).

In this study, an APCP equipment known as atmospheric pressure plasma jet was used. Different combinations of plasma power, plasma gas, and treatment time were tested on the inner surface of KN95 and FFP2 masks to disinfect them. *E. coli, Pseudomonas aeruginosa,* and different *Staphylococcus* spp. were evaluated.

The original contribution of this work was the determination of the optimal plasma treatment parameters to achieve a total inactivation of all bacteria while preserving the physical and morphological properties of the masks.

For this purpose, the antimicrobial activity of both plasma-treated and thermally treated inoculated samples was analyzed. In addition, plasma-treated samples were analyzed by scanning electron microscopy (SEM), visual evaluation, as well as filtration and breathing tests.

Materials and Methods

Sample masks

Mask disks (diameter 26 mm and 10 mm) and/or complete masks were used in this study (Figures 1-3). KN95 (Chinese standard: GB/T 32610-2016) masks were used for all microbiological analyses. However, from January 2021, KN95 masks were withdrawn from the Spanish market. Therefore, FFP2 (EN 149:2001; Certificate: 20/3212/00/0161; CE-0161FFP2) masks were used for the breathing and filtration analysis.

Plasma and thermal treatments

Different plasma treatments were applied to sets of three sample masks (Table 1). The APCP equipment used was PlasmaSpot500 (MPG, Luxemburg) for mask disks and complete mask treatments (Sainz-García *et al.*, 2021). It consists of one external electrode connected to a high voltage source, one internal grounded electrode, and an aluminum oxide (Al_2O_3) dielectric tube between them. Figures 2 and 3 illustrate the APCP equipment and how mask disks and complete masks were treated, respectively.

The effect of the heat flow generated by the plasma was studied by controlling the temperature during the plasma treatment and by applying thermal treatments in complete masks. The outer surface of the mask (layer 1) subjected to the best plasma treatment (nitrogen plasma 2 [N2]) was characterized by thermography using a thermal imaging camera (TESTO 871) (Testo SE & Co. KGaA, Germany). The obtained images were analyzed with the IRSoft (version 4.3) software. The temperature of the inner surface of the mask (layer 5) was monitored during each second of the 1.5 minutes of plasma treatment by a K-type Teflon-coated thermocouple connected to a data logger (Testo 167T4) (Figure 3c). This study was performed to determine the maximum temperature reached for each treatment. Heated gas thermal treatments were applied on inoculated complete masks to analyze the antimicrobial activity of the heat flow (Figure 3d).

Antimicrobial activity of plasma treatments on mask disks

Mask disks were inoculated with 10 µl of 0.5 McFarland suspension (10^8 Colony Forming Units/ml [CFU/ml]), performed in phosphate buffer saline (PBS, Gibco), of *E. coli* ATCC25922, *P. aeruginosa* PAO1, *S. aureus* ATCC29213, *Staphylococcus hominis* W220, *Staphylococcus haemolyticus* W1493, *Staphylococcus saprophyticus* W1498, *S. epidermidis* W213, *S. epidermidis* W232, *S. epidermidis* W1346, *S. aureus* W1623, and *S. aureus* W1570. The strains W213, W232, W1570, and W1623 presented a multidrug resistance phenotype (resistant to at least three families of antibiotics). Specifically, *S. epidermidis* W213 was resistant to beta-lactams, oxazolidinones, aminoglycosides, and phenicols; *S. epidermidis* W232 was resistant to beta-lactams, oxazolidinones, lincosamides, and aminoglycosides; *S. aureus* W1570 was resistant to beta-lactams, macrolides, lincosamides, aminoglycosides, and fluoroquinolones, and *S. aureus* W1623 was resistant to beta-lactams, aminoglycosides, and fluoroquinolones.

Three bacteria were inoculated per disk for each treatment as shown in Figure 2. Three inoculated disks were used for each plasma treatment, including the CT treatment (Table 1) to control bacterial growth (positive control, CT-positive). In addition,

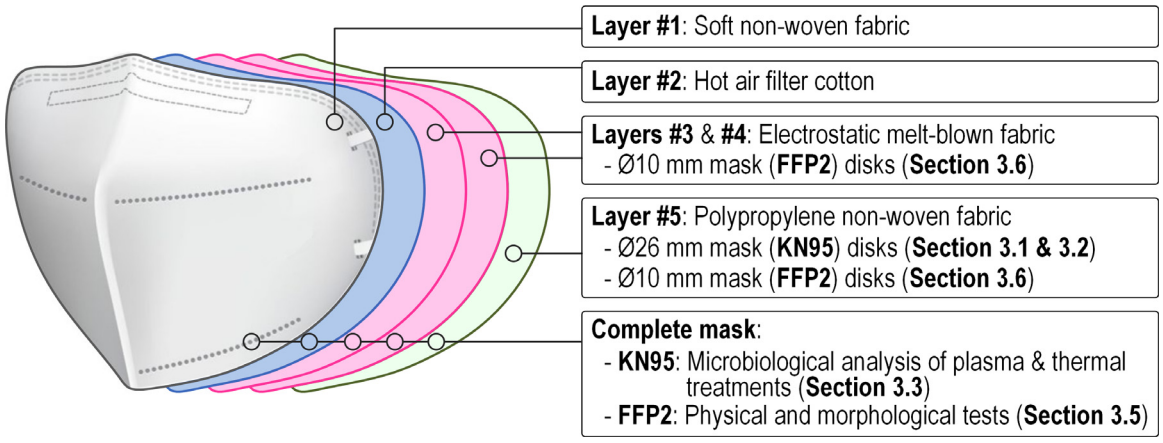

Figure 1. Scheme of the different layers of a mask (KN95 and FFP2) and description of masks used in each paper result section. FFP2 = filtering face piece 2.

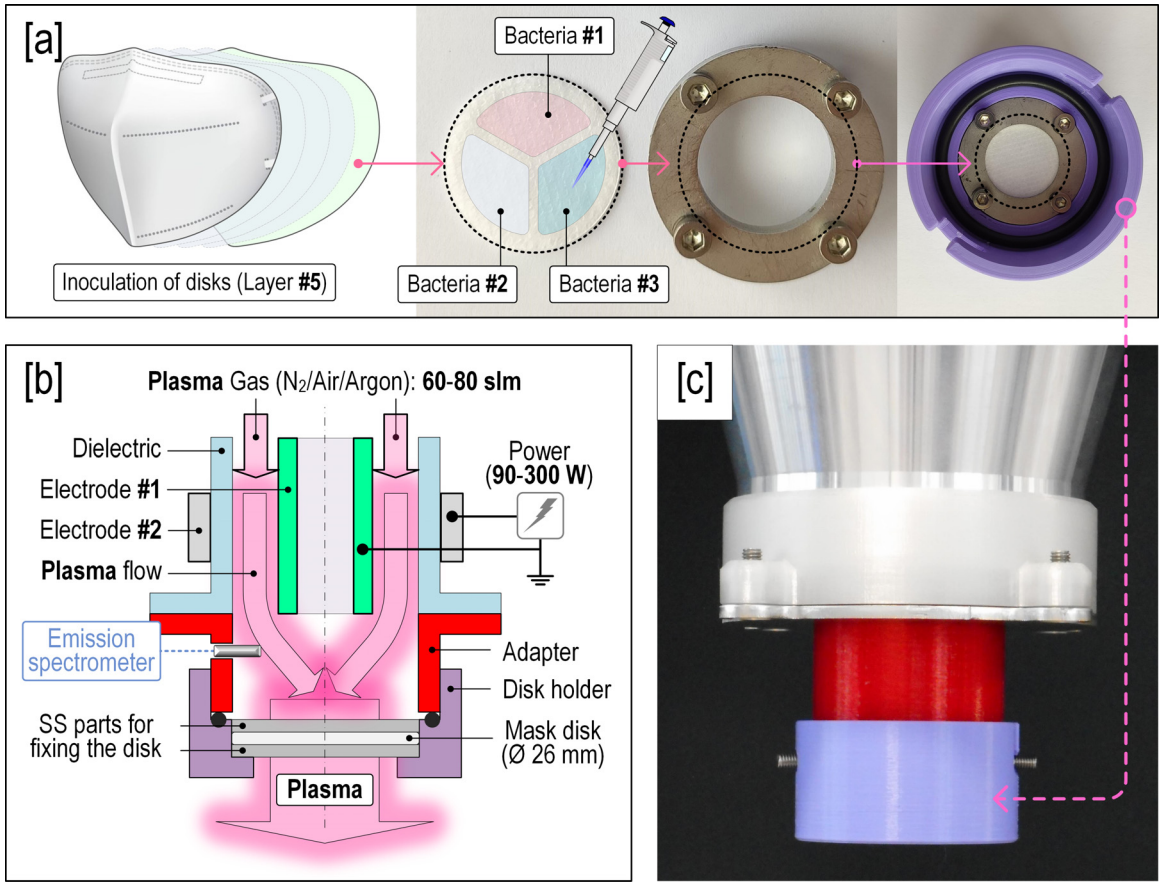

Figure 2. (a) KN95 mask from which Ø 26 mm disks were extracted. Disks and holders needed to treat the disks inoculated with *Escherichia coli* ATCC25922, *Staphylococcus aureus* ATCC29213, and *Pseudomonas aeruginosa* PAO1 suspensions; (b) Atmospheric pressure cold plasma equipment scheme; (c) Plasma equipment treating mask disks.

untreated disks without bacteria were used to analyze the presence of possible contaminants (negative control, CT-negative). No colonies were seen in the negative controls regardless of the treatment studied. Plasma treatments were applied after the inoculum was dry. Then, each inoculated area was independently washed in Eppendorf tubes with 300 µl of Mueller-Hinton broth (CondaLab) for 24 hours. After that, serial dilutions were performed and cultured in Brain Heart Infusion agar at 37° C overnight to determine the CFU/ml. Furthermore, the antimicrobial effect of the APCP treatments N2 and N3 was also analyzed by quantifying the fluorescence levels of the green fluorescent protein (GFP) in the *P. aeruginosa* strain ATCC15692GFP. For this purpose, mask disks were inoculated with 10 µl of *P. aeruginosa* ATCC15692GFP, dried, and then treated with APCP. GFP was quantified before and after the treatment by digital image analysis on a fluorescence microscope (Nikon) using the ImageJ software.

Antimicrobial activity of plasma treatments on complete masks

Five points were selected on the inner side of the masks (Nose-N; Mouth-M; Chin-CH, and both Cheeks-C1 and C2) as shown in Figure 3a. Each spot was inoculated with 10 µl of 0.5 McFar-

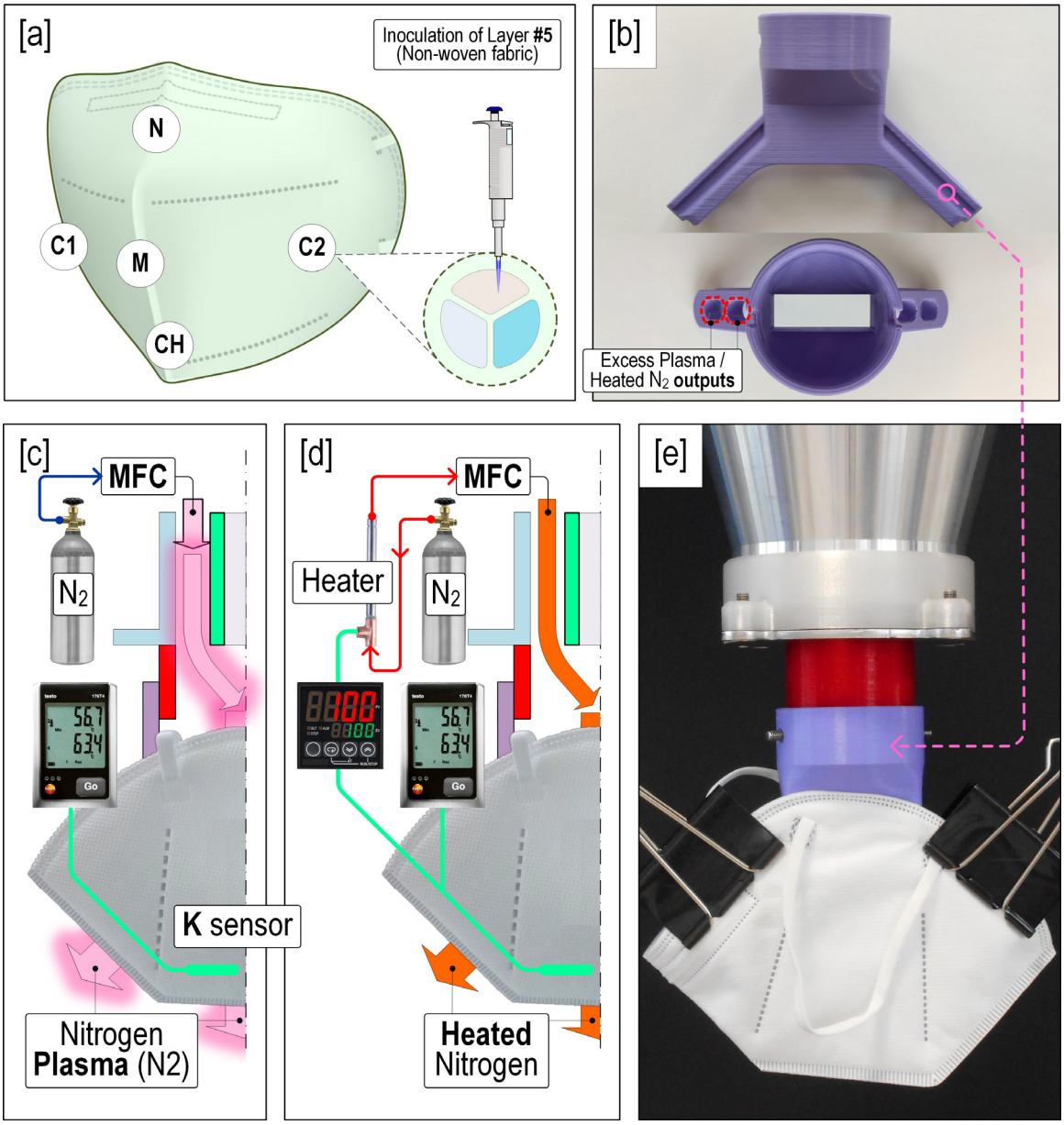

Figure 3. (a) Inoculation points on the inner layer of masks (Nose-N; Mouth-M; Chin-CH and both Cheeks-C1 and C2). Three bacteria were inoculated in each circle; (b) Mask holder; (c) and (d) Scheme of plasma and thermal treatments on masks; (e) Plasma equipment treating complete masks.

land suspension of *E. coli* ATCC25922, *S. aureus* ATCC29213, and *P. aeruginosa* PAO1. Three bacteria were inoculated per mask for each treatment. Untreated masks were used as positive controls for growth. Plasma treatment was applied after the inoculum was dried under sterile conditions. Subsequently, each area was cut and the viable bacteria CFU/ml were determined using the procedure described for mask disks.

Optical emission spectroscopy

Optical emission spectroscopy analysis was used to identify the RONS produced by N2, Ar1, and A2 plasma treatments (Table 1). The equipment used was the spectrometer F600-UVVIS-SR (StellarNet, Tampa, Florida, USA), connected to an optical fiber (QP600-2SR-Ocean Optics) with a lens that collected information of the plasma flux as shown in Figure 2b. Data were processed with the SpectraWiz software (StellarNet, Tampa, Florida, USA).

Physical and morphological characteristics of the mask after treatment

Filtration properties and breathing resistance of complete masks were measured by an external laboratory (AITEX, Spain). The filtration test was done by filter penetration with paraffin oil following the EN 149:2001+A1:2009 standard. The expanded uncertainty was ± 10% of the measured value for a 95% probability of coverage. The breathing resistance test was done following the same standard. In this case, the expanded uncertainty was ± 18% of the measured value for 95% probability of coverage. Each analysis was performed five times.

For morphological analysis, a HITACHI S-2400 SEM was used. Untreated and 5-time-plasma-treated (N2) (Table 1) mask disks from layers 4 and 5 were tested. Before SEM examination, mask disks were coated with a thin layer of gold and palladium, using a sputtering apparatus to make them conductive. In addition,

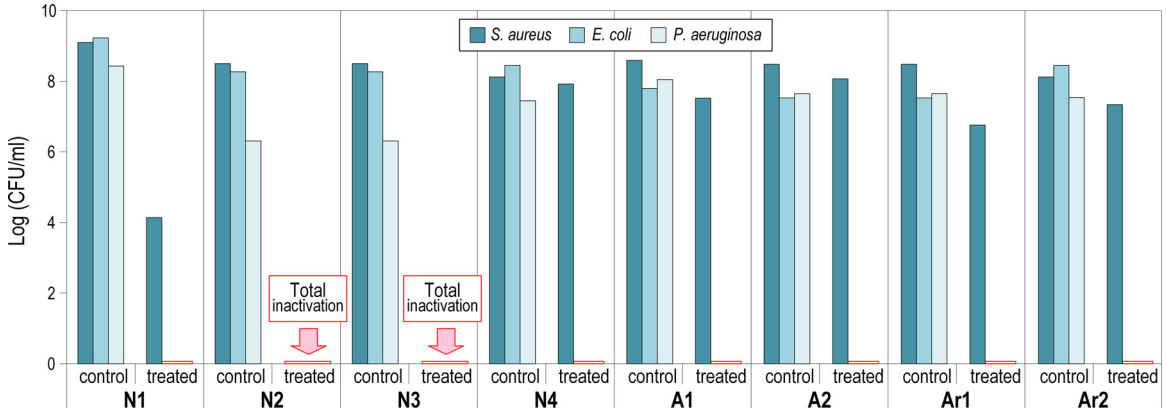

Figure 4. Comparison of antimicrobial activity of different plasma treatments and their controls in mask disksagainst *Staphylococcus aureus, Escherichia coli,* and *Pseudomonas aeruginosa*.

visual analysis was performed to detect any alterations in the treated masks.

Results and Discussion

Inactivation on mask disks by plasma treatments

The degree of bacterial inactivation was influenced by the bacterial species analyzed and the modification of the plasma treatment parameters. Figure 4 shows the antimicrobial activity of the plasma treatments against *E. coli* ATCC25922, *P. aeruginosa* PAO1, and *S. aureus* ATCC29213 on mask disks in comparison with the CT-positive.

The best treatments were the nitrogen plasma treatments (N2 and N3) as they achieved total inactivation regardless of the target bacteria. Furthermore, all studied treatments achieved complete inactivation of *E. coli* and *P. aeruginosa*, with *S. aureus* being the most resistant species, consistent with other studies (Han *et al.*, 2016; Huang *et al.*, 2020; Kayes *et al.*, 2007; Lunov *et al.*, 2016). For instance, Huang *et al.* (2020) and Han *et al.* (2016) found higher inactivation values in *Salmonella Typhimurium* and *E. coli*, respectively, than in *S. aureus* after plasma treatment of 96-well microtiter plates and Petri dishes, respectively (Han *et al.*, 2016; Huang *et al.*, 2020).

Several authors consider the morphological characteristics of bacteria as one of the factors responsible for the differences in bacterial inactivation (Huang *et al.*, 2020). Both Gram-positive and Gram-negative bacteria possess cell wall peptidoglycans, but Gram-positive bacteria have a thick peptidoglycan wall that allows them to resist plasma damage. Besides, other researchers have identified different action mechanisms depending on Gram-positive and Gram-negative bacteria. For Gram-positive bacteria, it has been suggested that RONS play the main role in provoking lipid membrane disturbances after lipid peroxidation of unsaturated fatty acids. Amino acid oxidation results in protein modification, followed by DNA damage and cell death (Arjunan *et al.*, 2015; Šimončicová *et al.*, 2018; Yong *et al.*, 2015). However, in the case of Gram-negative bacteria, with irregular surfaces, electrostatic disruption is the most effective effect (Lunov *et al.*, 2016; Mai-Prochnow *et al.*, 2016). This effect involves the rupture of the membrane when the outer membrane acquires sufficient electric charge. Regarding the bacteria analyzed in our work, *E. coli* and *P. aeruginosa* are Gram-negative bacteria, and *S. aureus* is Gram-positive, which could explain the differences in the inactivation rates.

In addition, plasma treatment time, power, or gas, influenced the bacterial inactivation results, as many authors have previously indicated (Han *et al.*, 2016; Huang *et al.*, 2020; Lunov *et al.*, 2016; Miao and Jierong, 2009; Surowsky *et al.*, 2014; Wiegand *et al.*, 2014). Han *et al.* (2016) demonstrated that the longer the exposure time, the higher the bacterial damage (Han *et al.*, 2016). This is in accordance with our results as N1 treatment (45 seconds) only achieved 4.96 log (CFU/ml) reductions, whereas N2 (1.5 minutes) or N3 (2.5 minutes), caused total inactivation. Although the treatment time for N4 plasme treatment was the longest (5 minutes), the plasma power was not enough to inactivate all bacteria (220 W). N2 treatment (300 W; 1.5 minutes) resulted in higher inactivation values than N4 (220 W; 5 minutes), indicating that treatment power plays a more important role than treatment time. In this regard, another previous study reported that when the power was increased from 75 W to 125 W, inactivation by plasma treatment against *L. monocytogenes, E. coli,* and *S. Typhimurium* also increased (Kim *et al.*, 2011). Plasma power provides energy to generate RONS. Thus, the higher the power, the larger the amount of RONS generated to inactivate the bacteria (Laroussi and Leipold, 2004; Lu *et al.*, 2016).

Finally, plasma gas played one of the main roles in terms of antimicrobial activity. Comparing the studied gases (nitrogen, air, and argon), the best was nitrogen because it achieved total inactivation regardless of the bacteria used.

The effect of N2 and N3 treatments against *P. aeruginosa* ATCC15692GFP was also studied by analyzing their antimicrobial activities and the fluorescence levels of GFP (Figure 5). This bacterium possesses a multicopy vector encoding the green fluorescent protein GFPmut3. Both plasma treatments achieved antimicrobial activity (> 7 logarithmic reductions, data not shown), and they also reduced protein concentration. GFP signals after N2 and N3 treatments were 43% and 54% respectively, in comparison with signal control (100%) with statistically significant differences ($p \leq 0.05$). Hence, it is confirmed that both treatments were effective against *P. aeruginosa* ATCC15692GFP.

Inactivation of different species of Staphylococcus

Staphylococcus species are one of the most important causes of nasopharyngeal infections and can be implicated in the most aggressive types of maskne (Daou *et al.*, 2021; Jusuf *et al.*, 2020; Revai *et al.*, 2008; Sun and Chang, 2017). For that reason, we investigated different *Staphylococcus* spp. strains (*S. hominis* W220, *S. haemolyticus* W1493, *S. saprophyticus* W1498, *S. epidermidis* W213, W232 and W1346, and *S. aureus* W1623 and W1570) from the clinical collection of Molecular Microbiology Area of the Biomedical Research Center of La Rioja (CIBIR), to determine their resistance to plasma treatment. Among them, the methicillin and linezolid-resistant

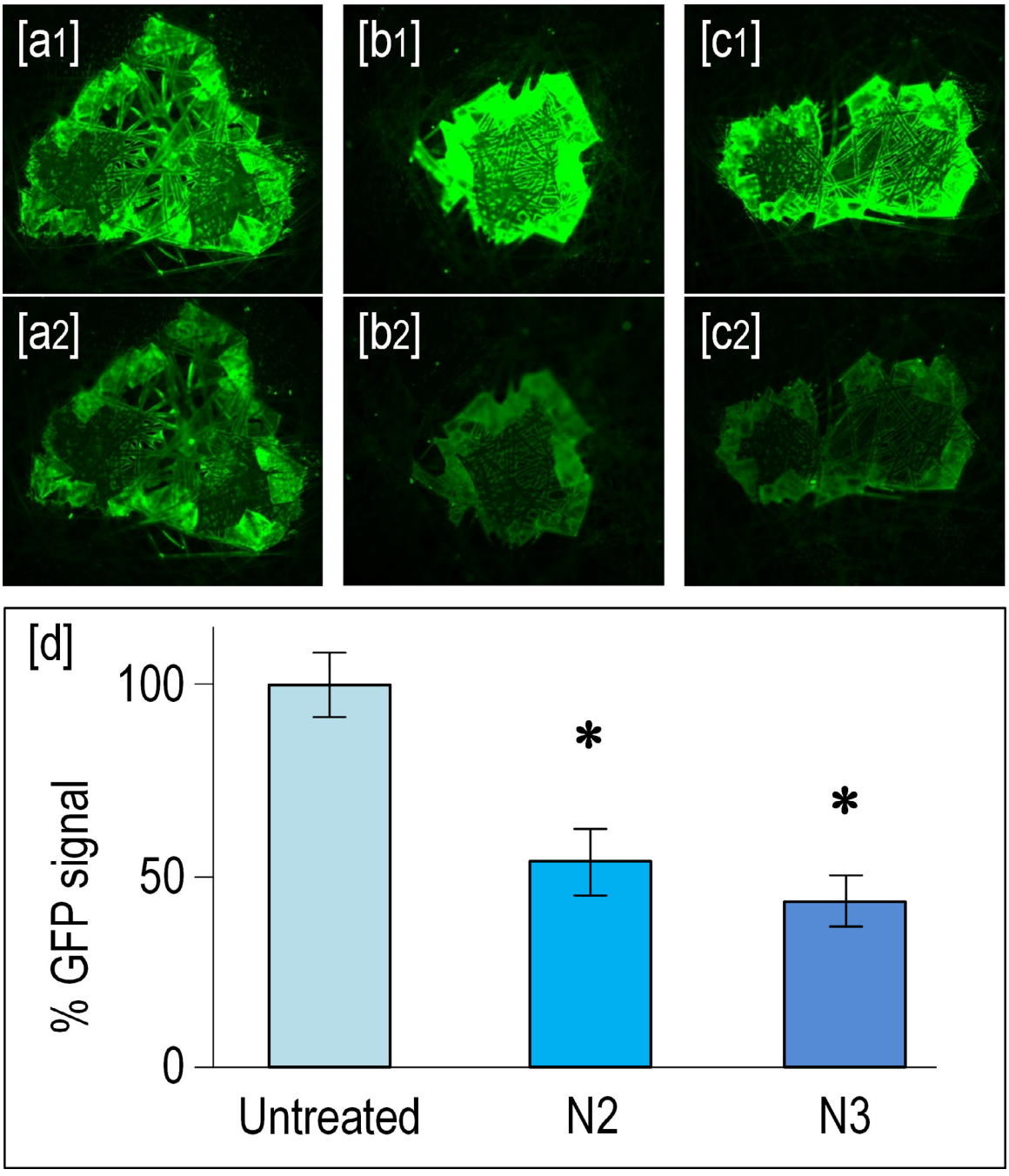

Figure 5. Fluorescence microscope digital images of GFP quantification: (a1, b1, and c1) before and (a2, b2, and c2) after CT, N2, and N3 plasma treatments, respectively; (d) GFP signal percentage of these treatments (*, $p \leq 0.05$).
GFP = green fluorescent protein.

S. epidermidis W213 and W232, and the methicillin-resistant *S. aureus* W1570 and W1623 presented multidrug-resistant phenotypes. Tests were performed applying the best plasma treatment identified in section 3.1 (N2) and following the same procedures. All strains, including the multidrug-resistant strains, were completely inactivated after 1.5 minutes of N2 treatment.

Inactivation of the complete mask by plasma and thermal treatments

N2 plasma treatment was chosen to study the antibacterial activity on complete masks as more than six logarithmic reductions were observed against *E. coli* ATCC25922, *S. aureus* ATCC29213, and *P. aeruginosa* PAO1 (Figure 4). In addition, the thermal effect was studied to determine the antimicrobial capacity associated with the flow of heat generated by the plasma.

On the one hand, the thermal images of the outer layer of the mask (layer 1) with the N2 treatment at different times showed a homogeneous thermal distribution (Figure 6), indicating a homogeneous plasma treatment. The temperatures on the outer surface of the mask at the end of the N2 treatment ranged from 80 °C to 90 °C (Figure 6d). On the other hand, the maximum temperature of the inner mouth zone of the mask during the N2 plasma treatment was 100 °C (Figure 7). This temperature was used as a guide to heat an 80 standard liter per minute -nitrogen flux using

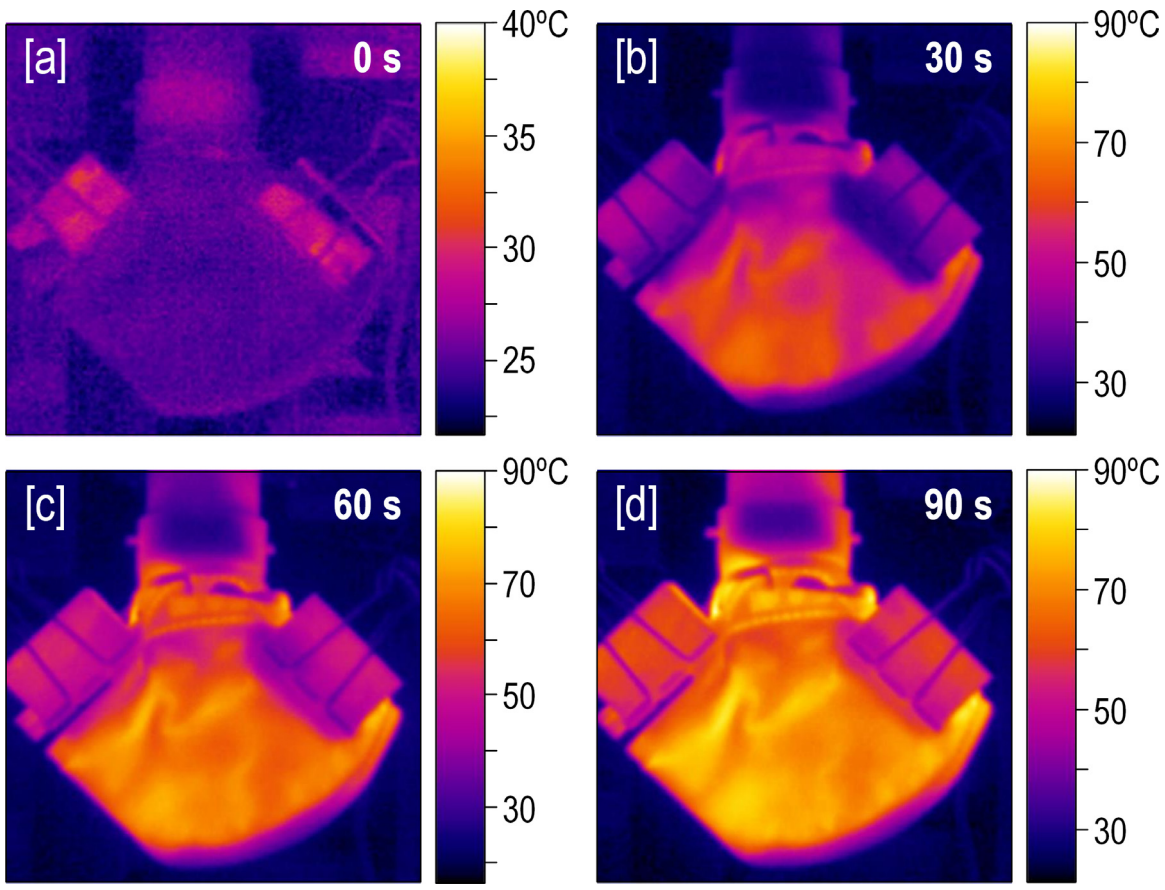

Figure 6. Mask outer surface thermography (layer 1) during N2 plasma treatment at different times: (a) 0 seconds, (b) 30 seconds, (c) 60 seconds, and (d) 90 seconds.

Table 1
Conditions of plasma treatments

Treatment code	Plasma Gas	Gas Flow (slm)	Cooling Gas	Plasma Power (W)	Treatment time
CT	-	-	-	-	-
N1	Nitrogen	80	Air	300	45 seconds
N2	Nitrogen	80	Air	300	1.5 minutes
N3	Nitrogen	80	Air	300	2.5 minutes
N4	Nitrogen	80	Air	220	5 minutes
A1	Air	80	Air	300	45 seconds
A2	Air	80	Air	300	1.5 minutes
Ar1	Argon	60	Air	90	1.5 minutes
Ar2	Argon	60	Air	60	5 minutes

slm, standard liter per minute.

Table 2
Comparison of the antimicrobial activity of plasma (N2) and thermal treatments against *S. aureus* ATCC29213, *E. coli* ATCC25922, and *P. aeruginosa* PAO1 inoculated in complete masks

Bacteria	Recuperated bacteria in control samples (control-positive)[a]		Recuperated bacteria after treatment (logarithmic reduction)[a]	
	CT	Thermal treatment	N2	Thermal treatment
Staphylococcus aureus ATCC29213	8.75	9.13	1.54 (7.21)	8.51 (0.62)
Escherichia coli ATCC25922	5.99	5.28	0 (5.99)	0 (5.28)
Pseudomonas aeruginosa PAO1	8.31	8.11	0 (8.31)	0 (8.11)

[a] The data are showed in log (CFU/ml).
CFU = colony forming units.

a thermal system controlled by a temperature regulator, and subsequently, each bacterium was subjected to that nitrogen flux for 1.5 minute. The thermal effect was the main cause of the inactivation of *P. aeruginosa* and *E. coli* as both treatments (plasma and heat flux) produced total inactivation of both bacteria (Table 2). However, heated flow was insufficient to inactivate *S. aureus,* and it could be affirmed that plasma treatment was necessary for the total inactivation of *S. aureus* in addition to heat flux treatment. To our knowledge, bacteria can be inactivated by a combination of several factors, including time and heat treatment. In this regard, some authors have studied how thermal treatment affects the inactivation of different bacteria (*P. aeruginosa* PAO1, *S. Typhimurium,*

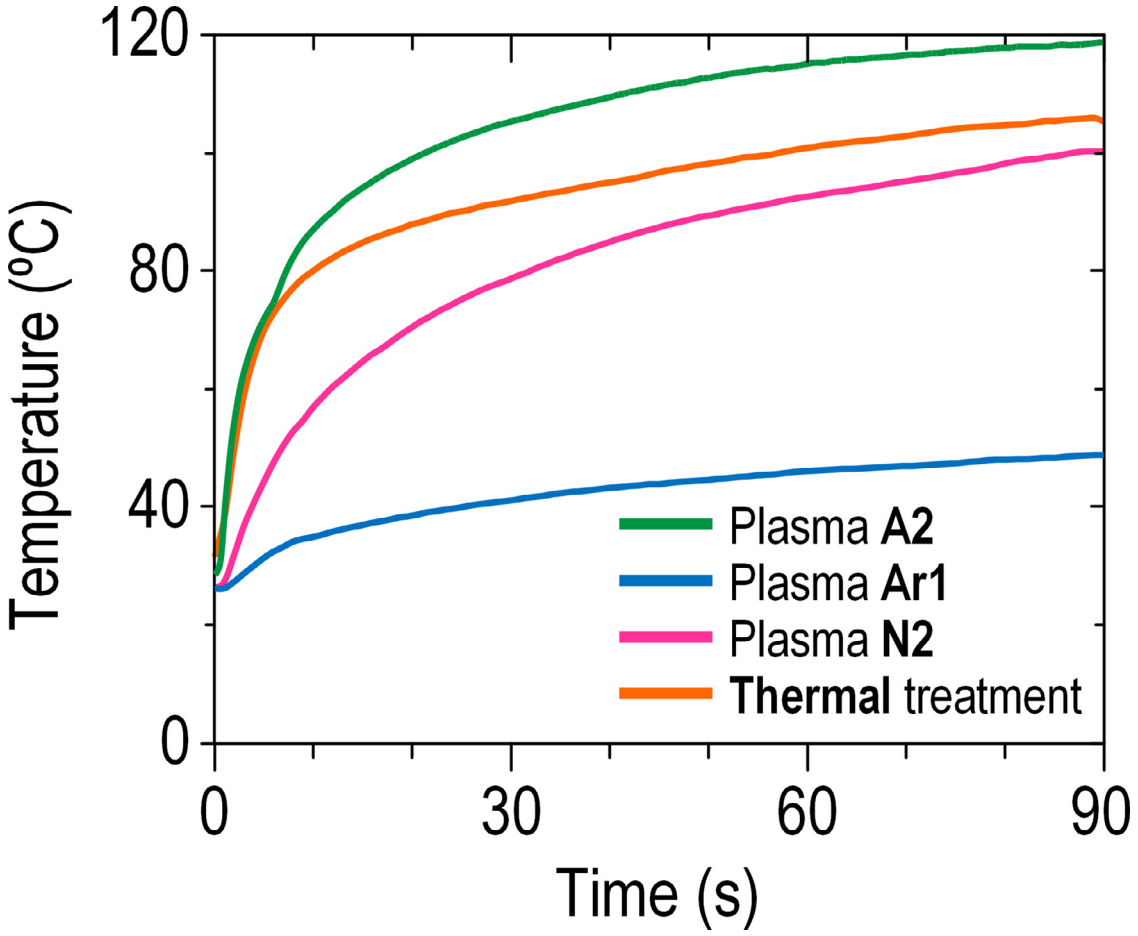

Figure 7. Temperature of the inner surface (layer 5) of a mask during plasma treatments (N2, Ar1, and A2) and thermal treatment measured by a type K thermocouple probe.

and *E. coli*) in different environments (sardinella meat, snail meat, and cells). They concluded that the higher the temperature and the time, the greater the bacteria reduction (Gabriel and Alano-Budiao, 2019; Gabriel and Ubana, 2007; Marcén *et al.*, 2017).

Optical emission spectroscopy

Figure 8 shows optical emission spectra (200-500 nm) of nitrogen, argon, and air plasma. It was possible to identify which relevant RONS appeared for each plasma gas and justify the antimicrobial activity. N2 treatment spectrum (Figure 8a) showed different species namely: (i) NO* radical (200-280 nm), (ii) Second positive system (SPS) of nitrogen (296-405 nm), and (iii) First negative system (FNS) of nitrogen (at 394 and 427 nm). SPS and FNS need to be taken into account because of their role in ozone (O_3) generation, a species with biocidal capacity and one that does not generate an excited state that emits light (Girgin Ersoy *et al.*, 2019; Marino *et al.*, 2018; Porto *et al.*, 2020; Wen *et al.*, 2020). O_3 generation is explained as follows (Kim *et al.*, 2021).

$$N_2 + e \rightarrow N_2^+ + e + e$$

$$N_2^+ + O_2 \rightarrow N_2^+ + O + O$$

$$O + O_2 + M \rightarrow O_3 + M$$

On the other hand, Ar1 (Figure 8b) showed the same species as N2, in addition to the OH* radical (309 nm). Finally, Figure 8c shows the spectrum of A2, where only the nitrogen species SPS and FNS were detected.

In this study, masks were treated using an assembly that conducts the plasma flow to the inner surface of the mask. Therefore, the combined antimicrobial effect of positive and negative ions, RONS, electrons, excited and neutral ions, heat, molecules, and UV photons can be leveraged (Scholtz *et al.*, 2015). Most authors propose that the effect of RONS is most likely responsible for the inactivation capacity of atmospheric pressure plasma jet (Iuchi *et al.*, 2018; Sainz-García *et al.*, 2021). In fact, it has been previously reported that the NO*, OH*, and O_3 species confirmed antimicrobial activity (Kaushik *et al.*, 2018; Laroussi and Leipold, 2004; Porto *et al.*, 2020; Wen *et al.*, 2020; Wu *et al.*, 2017; Zhang *et al.*, 2016).

The following conclusions might be drawn when comparing treatments: (i) N2 treatment achieved the best bacterial inactivation (Figure 4), and among all the reactive species identified, the NO* radical could be the most biocidal RONS, as it has the highest peak and intensity (Figure 8a). (ii) The antimicrobial capacity of Ar1 was similar to that of A2 despite generating a significantly lower heat flow than the other treatments (Figure 7). In this case, OH* radicals and O_3 from nitrogen species SPS and FNS seem to balance out the lower Ar1 inactivation effect due to the low temperature. (iii) Notwithstanding the lower relative intensities for all RONS (NO*, OH*, and O_3), the inactivation performed by treatment A2 could benefit from heat flux (highest temperature) (Figure 7).

Physical and morphological characteristics of the mask after treatment

Filtration capacity (FC), breathing resistance, visual modifications, and adaptability to the face were assessed after plasma

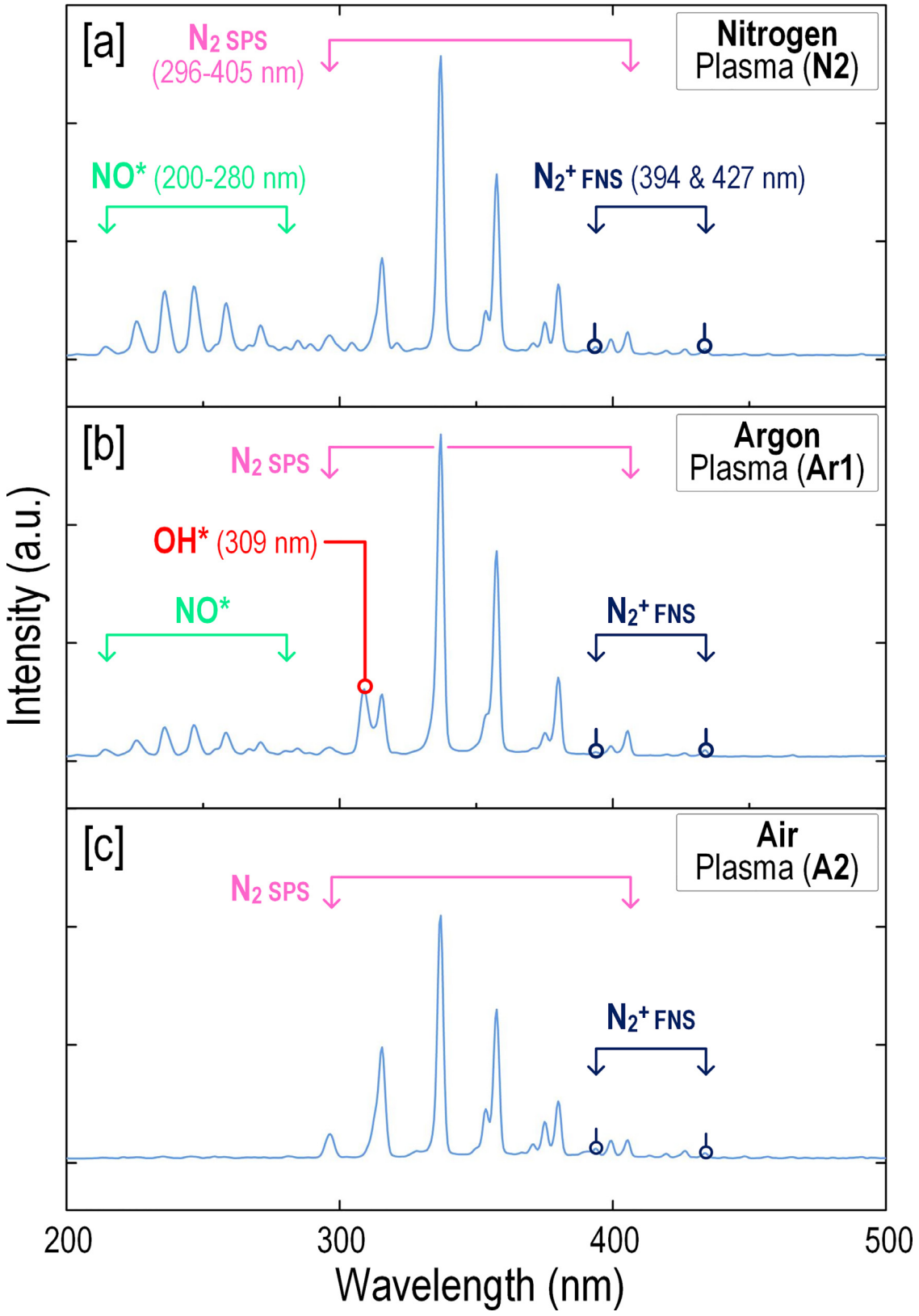

Figure 8. Optical emission spectra of plasma treatments: (a) nitrogen plasma N2, (b) argon plasma Ar1, and (c) air plasma A2.

Table 3
Filtration capacity and breathing resistance after one (KN95) and five (FFP2) treatment cycles

Type of mask		Resistance to inhalation (mbar)		Resistance to exhalation (mbar)	Paraffin oil penetration (%)
		30 l/min	95 l/min	160 l/min	
KN95	Control	0.387 ± 0.02	1.217 ± 0.05	2.160 ± 0.02	7.148 ± 0.31
	1 cycle	0.420 ± 0.01	1.350 ± 0.02	2.277 ± 0.09	7.135 ± 0.22
FFP2	Control	0.466 ± 0.03	2.020 ± 0.05	2.986 ± 0.01	1.418 ± 0.18
	5 cycles	0.410 ± 0.03	1.918 ± 0.05	2.954 ± 0.01	1.468 ± 0.21

FFP2 = filtering face piece 2.

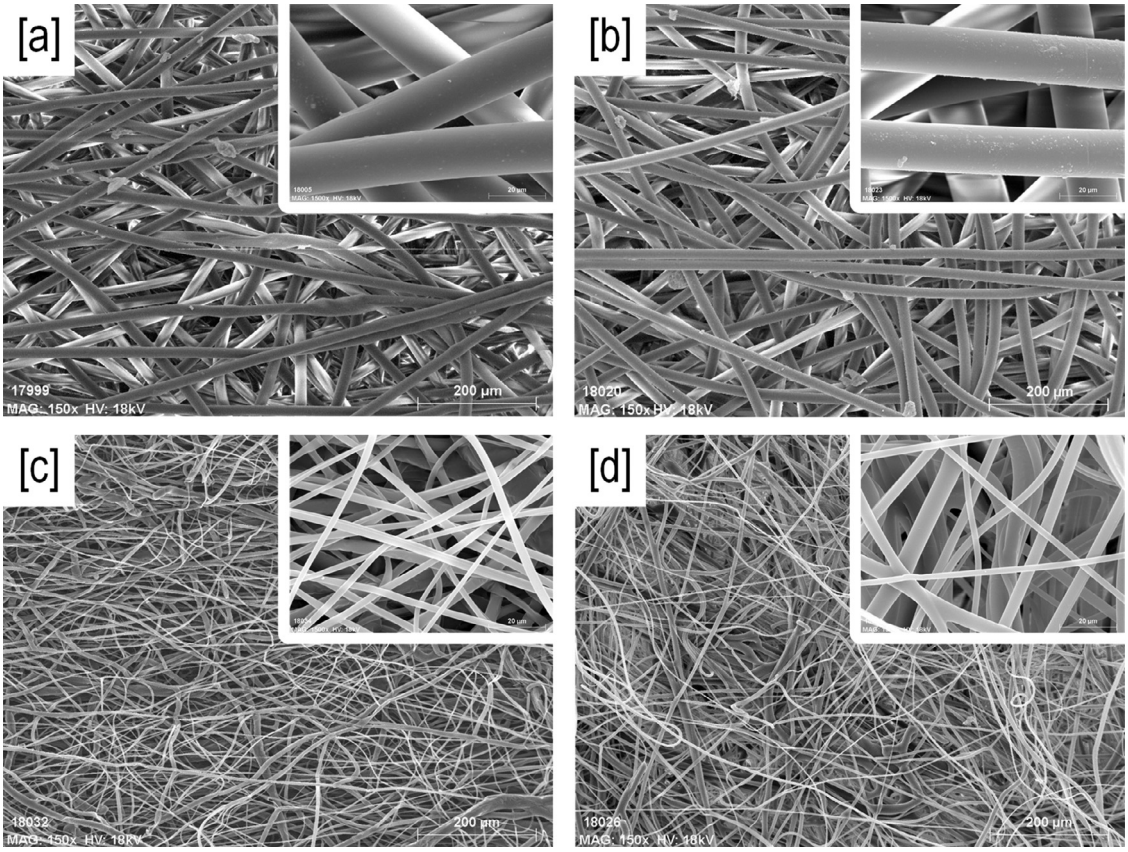

Figure 9. SEM images with a magnification of 150x and 1500x detail of samples: (a, c) Untreated layers 5 and 4, respectively, and (b, d) Layers 5 and 4 of a complete mask (FFP2) after five cycles of plasma treatment (N2).
FFP2 = filtering face piece 2; N2 = nitrogen plasma 2; SEM = scanning electron microscopy.

treatments. Table 3 shows FC and breathing resistance after one and five treatment cycles. Data obtained revealed that plasma treatment did not affect either breathing resistance or FC of masks for at least five treatment cycles. It was observed that the resistance to inhalation (30 l/minutes) increased from 0.387 mbar to 0.420 mbar after one cycle and decreased from 0.466 mbar to 0.410 mbar after five cycles, which were not significant differences. In contrast, in the study of inhalation 95 l/min and expiratory resistance, there was a slight increase in one cycle but a decrease after five cycles. Finally, the number of cycles did not affect the FC which was similar to the control masks. These results seem reasonable, and a slight increase in respiration implies a small decrease in FC. Nevertheless, this reduction could be neglected considering that FC of treated masks during five cycles only lost 3.4% of FC with regard to the control masks (FC = 1.418). Our study demonstrated that treated masks maintained a FC of 1.468, similar to FFP3 (FC = 1). These findings are in line with previous results that applied five cycles (60 seconds) of O_3 plasma treatment on masks without observing modifications in the structural characteristics, functional properties and inhalation resistance of the filter layer (Lee *et al.*, 2021). Moreover, previous studies observed no modification in the functional characteristics of masks after one cycle of plasma treatment, suggesting that after one cycle, it is possible to reuse masks in terms of FC and breathing resistance (Bergman *et al.*, 2010; Osaili *et al.*, 2020; Wigginton *et al.*, 2021). It is worth noting that we succeeded with five plasma treatment cycles, as few studies have evaluated more than one plasma treatment cycle without affecting the functional properties of the masks. Other researchers have studied the effect of more than one cycle of other decontamination technologies on the masks. Wigginton *et al.* (2021) demonstrated a maintained filtration efficacy and proper fit after 10 cycles of VHP and moist heat (Wigginton *et al.*, 2021). Bergman *et al.* (2010) showed no differences in FC with three cycles of UV, ethylene oxide or microwaves (Bergman *et al.*, 2010). Other authors applied 10 cycles of either ozone or steam and 20 cycles of microwaves without affecting filtration efficiency (Blanco *et al.*, 2021; Ou *et al.*, 2020; Zulauf *et al.*, 2020).

Furthermore, it was observed that the plasma treatment applied in this research had no impact on the mechanical and face comfort capacity as well as visual modifications. There were no

differences between control masks and treated masks: no fragmented or stretched elastic trips and no degradation in mask color (data not shown). On the contrary, Viscusi *et al.* (2009) observed that metallic nosebands were tarnished and not as shiny as in the control masks after a 55-minute plasma treatment.

SEM analysis

Layers 5 and 4 from untreated and plasma-treated samples (five cycles) were analyzed with SEM to determine the possible impact of plasma on surface morphology. SEM images of the samples with a magnification of 150x and 1500x, showed no differences (Figure 9). These results demonstrated no negative impact on the fibers of the treated masks, which is probably related to the fact that their FC was maintained. Therefore, it can be concluded that plasma treatment can be applied without provoking a noticeable damage on mask surfaces.

Conclusions

Due to the COVID-19 pandemic, mask-wearing has increased over the last few years. In this scenario, there has also been a huge increase in facial diseases caused by masks. In addition, there is a shortage of masks due to massive use. In this regard, in this study we investigated the effectiveness of an atmospheric pressure plasma jet equipment in disinfecting masks and maintaining their functional properties. It is worth mentioning that, to the best of our knowledge, this is the first study in which a complete FFP2 mask was disinfected using APCP. Our results suggested that plasma power, plasma gas, and treatment time must be considered to determine the degree of bacterial inactivation. The longer the treatment time and plasma power, the higher the inactivation. Regardless of the type of bacteria, the use of nitrogen plasma, 300 W power, and 1.5 minutes of treatment were the optimal plasma parameters for total inactivation of bacteria. Furthermore, the thermal study confirmed that both *P. aeruginosa* PAO1 and *E. coli* ATCC25922 were inactivated mainly by means of the thermal effect. In contrast, RONS generated in plasma were the main cause of *Staphylococcus* inactivation. Specifically, NO* radical seems to be the most biocidal radical.

FC, breathing resistance analysis and SEM images confirmed that neither reduction in FC nor morphological modifications occurred in the masks even after five cycles of plasma treatment. In conclusion, disinfection of used masks with APCP could be an emergency solution to reduce facial infections and to solve mask shortages as well as the environmental problems associated with discarding masks. Moreover, this disinfecting technology could be applied to other objects and personal protective equipment used in hospitals.

Funding

This research did not receive any specific grant from funding agencies in the public, commercial, or not-for-profit sectors.

Ethical approval

Not applicable since this was a laboratory study not involving any clinical samples or human and animal subjects.

Author contributions

Ana Sainz-García: Study design, Data collection, Data analysis, Writing-Original Draft, Review & Editing, Visualization, Supervision. **Paula Toledano:** Study design, Data collection, Data analysis, Writing-Review & Editing. **Ignacio Muro-Fraguas:** Study design, Data collection, Data analysis, Writing-Review & Editing. **Lydia Álvarez-Erviti:** Data collection, Data analysis, Writing-Review & Editing. **Rodolfo Múgica-Vidal:** Study design, Data collection, Data analysis, Writing-Review & Editing. **María López:** Study design, Data collection, Data analysis, Writing-Review & Editing. **Elisa Sainz-García:** Study design, Data collection, Data analysis, Writing-Original Draft, Review & Editing. **Beatriz Rojo-Bezares:** Study design, Data collection, Data analysis, Writing-Review & Editing. **Yolanda Sáenz:** Study design, Data collection, Data analysis, Resources, Writing-Review & Editing, Supervision. **Fernando Alba-Elías:** Study design, Data collection, Data analysis, Resources, Writing-Review & Editing, Supervision.

Data availability statement

Data that support the findings of this study are available from the corresponding author upon reasonable request.

Declaration of competing interest

The authors have no competing interests to declare.

Acknowledgments

The authors wish to thank Dr. Francesco Tampieri (Universitat Politécnica de Catalunya) for his support in the optical emission spectra acquisition. This publication is based upon work from COST Action CA20114 PlasTHER, supported by COST (European Cooperation in Science and Technology-www.cost.eu). The author Elisa Sainz-García, as a postdoctoral researcher of the University of La Rioja, thanks the postdoctoral training program funded by the Plan Propio of the University of La Rioja. Authors Ignacio Muro-Fraguas and Ana Sainz-García are thankful to the program of pre-doctoral contracts for the training of research staff funded by the University of La Rioja and Spanish Ministry of Science and Innovation, respectively.

References

Arjunan KP, Sharma VK, Ptasinska S. Effects of atmospheric pressure plasmas on isolated and cellular DNA-a review. Int J Mol Sci 2015;16:2971–3016.
Bao L, Zhang C, Dong J, Zhao L, Li Y, Sun J. Oral microbiome and SARS-CoV-2: beware of lung co-infection. Front Microbiol 2020;11:1840.
Battelle. Bioquell hydrogen peroxide vapor (HPV) decontamination for reuse of N95 respirators. Columbus: FDA 2016:1–46.
Bergman MS, Viscusi DJ, Heimbuch BK, Wander JD, Sambol AR, Shaffer RE. Evaluation of multiple (3-Cycle) decontamination processing for filtering facepiece respirators. J Eng Fibers Fabr 2010;5:33–41.
Blanco A, Ojembarrena FB, Clavo B, Negro C. Ozone potential to fight against SAR-COV-2 pandemic: facts and research needs. Environ Sci Pollut Res Int 2021;28:16517–31.
Cassorla L. Decontamination and reuse of N95 filtering facepiece respirators: where do we stand? Anesth Analg 2021;132:2–14.
Catching A, Capponi S, Te YM, Bianco S, Andino R, Francisco S, et al. Graduate program in biophysics, University of California, San Francisco, San Francisco, CA **industrial and applied genomics, AI and cognitive software**. San Francisco: IBM Almaden Research Center; 2021.
Choi SY, Hong JY, Kim HJ, Lee GY, Cheong SH, Jung HJ, et al. Mask-induced dermatoses during the COVID-19 pandemic: a questionnaire-based study in 12 Korean hospitals. Clin Exp Dermatol 2021;46:1504–10.
Damiani G, Gironi LC, Grada A, Kridin K, Finelli R, Buja A, et al. COVID-19 related masks increase severity of both acne (maskne) and rosacea (mask rosacea): multi-center, real-life, telemedical, and observational prospective study. Dermatol Ther 2021;34:e14848.
Daou H, Paradiso M, Hennessy K, Seminario-Vidal L. Rosacea and the microbiome: a systematic seview. Dermatol Ther (Heidelb) 2021;11:1–12.
Dharmaraj S, Ashokkumar V, Hariharan S, Manibharathi A, Show PL, Chong CT, et al. The COVID-19 pandemic face mask waste: a blooming threat to the marine environment. Chemosphere 2021;272.
Feng S, Shen C, Xia N, Song W, Fan M, Cowling BJ. Rational use of face masks in the COVID-19 pandemic. Lancet Respir Med 2020;8:434–6.
Fischer RJ, Morris DH, Van Doremalen N, Sarchette S, Matson MJ, Bushmaker T, et al. Effectiveness of N95 respirator decontamination and reuse against SARS-CoV-2 Virus. Emerg Infect Dis 2020;26:2253–5.

Gabriel AA, Alano-Budiao AS. Thermal inactivation of *Pseudomonas aeruginosa* 1244 in salted *Sardinella fimbriata* meat homogenate. Agr Nat Resour 2019;53:79–83.
Gabriel AA, Ubana MA. Decimal reduction times of Salmonella Typhimurium in guinataang kuhol: an indigenous Filipino dish. LWT Food Sci Technol 2007;40:1108–11.
Girgin Ersoy Z, Barisci S, Dinc O. Mechanisms of the Escherichia coli and Enterococcus faecalis inactivation by ozone. LWT 2019;100:306–13.
Han L, Patil S, Boehm D, Milosavljević V, Cullen PJ, Bourke P. Mechanisms of inactivation by high-voltage atmospheric cold plasma differ for Escherichia coli and Staphylococcus aureus. Appl Environ Microbiol 2016;82:450–8.
Heimbuch BK, Wallace WH, Kinney K, Lumley AE, Wu CY, Woo MH, et al. A pandemic influenza preparedness study: use of energetic methods to decontaminate filtering facepiece respirators contaminated with H1N1 aerosols and droplets. Am J Infect Control 2011;39:e1–9.
Hua W, Zuo Y, Wan R, Xiong L, Tang J, Zou L, et al. Short-term skin reactions following use of N95 respirators and medical masks. Contact Dermatitis 2020;83:115–21.
Huang M, Zhuang H, Zhao J, Wang J, Yan W, Zhang J. Differences in cellular damage induced by dielectric barrier discharge plasma between Salmonella typhimurium and Staphylococcus aureus. Bioelectrochemistry 2020;132.
Ibáñez-Cervantes G, Bravata-Alcántara JC, Nájera-Cortés AS, Meneses-Cruz S, Delgado-Balbuena L, Cruz-Cruz C, et al. Disinfection of N95 masks artificially contaminated with SARS-CoV-2 and ESKAPE bacteria using hydrogen peroxide plasma: impact on the reutilization of disposable devices. Am J Infect Control 2020;48:1037–41.
Iuchi K, Morisada Y, Yoshino Y, Himuro T, Saito Y, Murakami T, et al. Cold atmospheric-pressure nitrogen plasma induces the production of reactive nitrogen species and cell death by increasing intracellular calcium in HEK293T cells. Arch Biochem Biophys 2018;654:136–45.
Jusuf NK, Putra IB, Sari L. Differences of microbiomes found in non-inflammatory and inflammatory lesions of acne vulgaris. Clin Cosmet Investig Dermatol 2020;13:773–80.
Kaushik NK, Ghimire B, Li Y, Adhikari M, Veerana M, Kaushik N, et al. Biological and medical applications of plasma-activated media, water and solutions. Biol Chem 2018;400:39–62.
Kayes MM, Critzer FJ, Kelly-Wintenberg K, Roth JR, Montie TC, Golden DA. Inactivation of foodborne pathogens using a one atmosphere uniform glow discharge plasma. Foodborne Pathog Dis 2007;4:50–9.
Kenney PA, Chan BK, Kortright KE, Cintron M, Russi M, Epright J, et al. Hydrogen peroxide vapor decontamination of N95 respirators for reuse. Infect Control Hosp Epidemiol 2020;43:45–7.
Kim B, Yun H, Jung S, Jung Y, Jung H, Choe W, et al. Effect of atmospheric pressure plasma on inactivation of pathogens inoculated onto bacon using two different gas compositions. Food Microbiol 2011;28:9–13.
Kim M, Lawson J, Hervé R, Jakob H, Ganapathisubramani B, Keevil CW. Development of a rapid plasma decontamination system for decontamination and reuse of filtering facepiece respirators. AIP Adv 2021;11.
Kumar A, Kasloff SB, Leung A, Cutts T, Strong JE, Hills K, et al. N95 mask decontamination using standard hospital sterilization technologies. MedRxiv 20 April 2020 (accessed 29 August 2022). doi:10.1101/2020.04.05.20049346.
Kutlu Ö, Güneş R, Coerdt K, Metin A, Khachemoune A. The effect of the "stay-at-home" policy on requests for dermatology outpatient clinic visits after the COVID-19 outbreak. Dermatol Ther 2020;33:e13581.
Laroussi M, Leipold F. Evaluation of the roles of reactive species, heat, and UV radiation in the inactivation of bacterial cells by air plasmas at atmospheric pressure. Int J Mass Spectrom 2004;233:81–6.
Lee J, Bong C, Lim W, Bae PK, Abafogi AT, Baek SH, et al. Fast and easy disinfection of coronavirus-contaminated face masks using ozone gas produced by a dielectric barrier discharge plasma generator. Environ Sci Technol Lett 2021;8:339–44.
Lin TH, Chen CC, Huang SH, Kuo CW, Lai CY, Lin WY. Filter quality of electret masks in filtering 14.6–594 nm aerosol particles: effects of five decontamination methods. PLoS One 2017;12.
Lin TH, Tang FC, Hung PC, Hua ZC, Lai CY. Relative survival of Bacillus subtilis spores loaded on filtering facepiece respirators after five decontamination methods. Indoor Air 2018;28:754–62.
Lore MB, Heimbuch BK, Brown TL, Wander JD, Hinrichs SH. Effectiveness of three decontamination treatments against influenza virus applied to filtering facepiece respirators. Ann Occup Hyg 2012;56:92–101.
Lu X, Naidis GV, Laroussi M, Reuter S, Graves DB, Ostrikov K. Reactive species in non-equilibrium atmospheric-pressure plasmas: generation, transport, and biological effects. Phys Rep 2016;630:1–84.
Lunov O, Zablotskii V, Churpita O, Jäger A, Polívka L, Syková E, et al. The interplay between biological and physical scenarios of bacterial death induced by non-thermal plasma. Biomaterials 2016;82:71–83.
Mai-Prochnow A, Clauson M, Hong J, Murphy AB. Gram positive and Gram negative bacteria differ in their sensitivity to cold plasma. Sci Rep 2016;6:38610.
Marcén M, Ruiz V, Serrano MJ, Condón S, Mañas P. Oxidative stress in E. coli cells upon exposure to heat treatments. Int J Food Microbiol 2017;241:198–205.
Marino M, Maifreni M, Baggio A, Innocente N. Inactivation of foodborne bacteria biofilms by aqueous and gaseous ozone. Front Microbiol 2018;9:2024.
Miao H, Jierong C. Inactivation of Escherichia coli and properties of medical poly(vinyl chloride) in remote-oxygen plasma. Appl Surf Sci 2009;255:5690–7.
Mills D, Harnish DA, Lawrence C, Sandoval-Powers M, Heimbuch BK. Ultraviolet germicidal irradiation of influenza-contaminated N95 filtering facepiece respirators. Am J Infect Control 2018;46:e49–55.
Mutalik SD, Inamdar AC. Mask-induced psoriasis lesions as Köebner phenomenon during COVID-19 pandemic. Dermatol Ther 2020;33:e14323.
Ng K, Poon BH, Kiat Puar TH, Shan Quah JL, Loh WJ, Wong YJ, et al. COVID-19 and the risk to health care workers: a case report. Ann Intern Med 2020;172:766–7.
Osaili TM, Hasan F, Dhanasekaran DK, Obaid RS, Al-Nabulsi AA, Rao S, et al. Thermal inactivation of Escherichia coli O157:H7 strains and Salmonella spp. in camel meat burgers. LWT 2020;120.
Ou Q, Pei C, Kim SC, Belani K, Faizer R, Bischof J, et al. COVID-19 pandemic—decontamination of respirators and masks for the general public, health care workers, and hospital environments. Anesthesia Patient Saf Foundation 2020;35:33–68.
Porto E, Alves Filho EG, Silva LMA, Fonteles TV, do Nascimento RBR, Fernandes FAN, et al. Ozone and plasma processing effect on green coconut water. Food Res Int 2020;131.
Revai K, Mamidi D, Chonmaitree T. Association of nasopharyngeal bacterial colonization during upper respiratory tract infection and the development of acute otitis media. Clin Infect Dis 2008;46:e34–7.
Sainz-García A, González-Marcos A, Múgica-Vidal R, Muro-Fraguas I, Escribano–Viana R, González-Arenzana L, et al. Application of atmospheric pressure cold plasma to sanitize oak wine barrels. LWT 2021;139.
Sangkham S. Face mask and medical waste disposal during the novel COVID-19 pandemic in Asia. Case Stud Chem Environ Eng 2020;2.
Scholtz V, Pazlarová J, Soušková H, Khun J, Julák J. Nonthermal plasma - a tool for decontamination and disinfection. Biotechnol Adv 2015;33:1108–19.
Šimončicová J, Kaliňáková B, Kováčik D, Medvecká V, Lakatoš B, Kryštofová S, et al. Cold plasma treatment triggers antioxidative defense system and induces changes in hyphal surface and subcellular structures of Aspergillus flavus. Appl Microbiol Biotechnol 2018;102:6647–58.
Smith JS, Hanseler H, Welle J, Rattray R, Campbell M, et al. 2020;3:7.
Suess T, Remschmidt C, Schink SB, Schweiger B, Nitsche A, Schroeder K, et al. The role of facemasks and hand hygiene in the prevention of influenza transmission in households: results from a cluster randomised trial; Berlin, Germany, 2009–2011. BMC Infect Dis 2012;12:26.
Sun KL, Chang JM. Special types of folliculitis which should be differentiated from acne. Dermatoendocrinol 2017;9.
Surowsky B, Fröhling A, Gottschalk N, Schlüter O, Knorr D. Impact of cold plasma on Citrobacter freundii in apple juice: inactivation kinetics and mechanisms. Int J Food Microbiol 2014;174:63–71.
Viscusi DJ, Bergman MS, Eimer BC, Shaffer RE. Evaluation of five decontamination methods for filtering facepiece respirators. Ann Occup Hyg 2009;53:815–27.
Wei J, Guo S, Long E, Zhang L, Shu B, Guo L. Why does the spread of COVID-19 vary greatly in different countries? Revealing the efficacy of face masks in epidemic prevention. Epidemiol Infect 2021;149:e24.
Wen G, Liang Z, Xu X, Cao R, Wan Q, Ji G, et al. Inactivation of fungal spores in water using ozone: kinetics, influencing factors and mechanisms. Water Res 2020;185.
Wiegand C, Beier O, Horn K, Pfuch A, Tölke T, Hipler UC, et al. Antimicrobial impact of cold atmospheric pressure plasma on medical critical yeasts and bacteria cultures. Skin Pharmacol Physiol 2014;27:25–35.
Wigginton KR, Arts PJ, Clack HL, Fitzsimmons WJ, Gamba M, Harrison KR, et al. Validation of N95 filtering facepiece respirator decontamination methods available at a large University Hospital. Open Forum Infect Dis 2021;8:ofaa610.
Wu S, Zhang Q, Ma R, Yu S, Wang K, Zhang J, et al. Reactive radical-driven bacterial inactivation by hydrogen-peroxide-enhanced plasma-activated-water. Eur Phys J Spec Top 2017;226:2887–99.
Yong HI, Kim HJ, Park S, Kim K, Choe W, Yoo SJ, et al. Pathogen inactivation and quality changes in sliced cheddar cheese treated using flexible thin-layer dielectric barrier discharge plasma. Food Res Int 2015;69:57–63.
Zhang Q, Ma R, Tian Y, Su B, Wang K, Yu S, et al. Sterilization efficiency of a novel electrochemical disinfectant against Staphylococcus aureus. Environ Sci Technol 2016;50:3184–92.
Zulauf KE, Green AB, Nguyen Ba ANN, Jagdish T, Reif D, Seeley R, et al. Microwave–generated steam decontamination of N95 respirators utilizing universally accessible materials. mBio 2020;11:1–9.